Correlation and confinement induced itinerant ferromagnetism in chain structures

Réka Trencsényi[a], Endre Kovács[b], and Zsolt Gulácsi[a]

[(a)] *Department of Theoretical Physics,*

University of Debrecen, H-4010 Debrecen, Hungary

[(b)] *Department of Physics, University of Miskolc,*

H-3515 Miskolc-Egyetemvaros, Hungary

(Dated: June 1, 2009)

Abstract

Using a positive semidefinite operator technique one deduces exact ground states for a zig-zag hexagon chain described by a non-integrable Hubbard model with on-site repulsion. Flat bands are not present in the bare band structure, and the operators $\hat{B}^{\dagger}_{\mu,\sigma}$ introducing the electrons into the ground state, are all extended operators and confined in the quasi 1D chain structure of the system. Consequently, increasing the number of carriers, the $\hat{B}^{\dagger}_{\mu,\sigma}$ operators become connected i.e. touch each other on several lattice sites. Hence the spin projection of the carriers becomes correlated in order to minimize the ground state energy by reducing as much as possible the double occupancy leading to a ferromagnetic ground state. This result demonstrates in exact terms in a many-body frame that the conjecture made at two-particle level by G. Brocks et al. [Phys.Rev.Lett. **93**,146405, (2004)] that the Coulomb interaction is expected to stabilize correlated magnetic ground states in acenes is clearly viable, and opens new directions in the search for routes in obtaining organic ferromagnetism. Due to the itinerant nature of the obtained ferromagnetic ground state, the systems under discussion may have also direct application possibilities in spintronics.

I. INTRODUCTION

A. Conducting chains

Conducting chains have been extensively studied in the past period, due to several reasons. First, periodic chains holding different type of cells are genuine objects for applications in device design techniques at the level of molecular nanotechnology[1]. As such, these systems represent a starting point in creating functional devices, materials and components on a 1-100 nanometer length scale which can lead to new routes in realizing functions of practical interest like field effect transistors, electroluminiscent diodes, nanocatalysis, hydrogen storage, etc.[2]. Second, several type of periodic conducting chains are in fact organic materials. Their nature, besides the fact that potentially allows developments that can lead to condensates on a plastic (as plastic ferromagnetism for example[3]), has exceptional qualities for new developments in electronics, for example in the direction of organic optoelectronic and field effect transistor components[4], high performance transistors and circuits made based on soluble materials[5], biodegradable devices used for controlled-release drug delivery inside of the human body[6], or electronic components on plastic providing flexible electronics[7]. Third, conducting chains exhibit quite interesting properties and phases important in advanced technological applications (as spintronics), for example insulating, conducting, half metallic, paramagnetic or ferromagnetic behavior[8]. Furthermore, these systems have the virtue of having fundamentally different ground states which can be tuned by external parameters like external fields or site selective gate potentials[9], opening new routes for the design of valves, switches, or control devices. Finally, the majority of conducting chains being described by non-integrable models, represent genuine challenges to theory and necessitate the development of rigorous techniques to describe the physical properties of these systems.

The chains under consideration are built up in fact from periodic arrangements of rings. Their theoretical study goes back to middle nineties and starts with triangular chains[10,11,12]. This case attracted attention especially by the study of the emergence possibilities of ferromagnetism in such systems[13,14], analysis of the stability of this phase[15], low temperature thermodynamics[16], numerical studies in two band cases[17], or even study of exact ground states in non-integrable situations[9].

The attempts to characterize the physical properties of quadrilateral chains have been

started later, being intensified by the study of Aharonov-Bohm cage properties[18], and have led to the description of quite interesting ground state characteristics in the diamond chain case which are tunable by external fields providing for example correlated half metal behavior applicable for spin-valve design[8].

The study of chains of pentagons intensified after 2000, when A. Heeger, A. MacDiarmid and H. Shirakawa obtained the Nobel prize in chemistry for the discovery and development of conducting polymers. The most common representatives of this class of materials are based on polythiophene, polypyrrole and polytriazole, all containing pentagon rings. The study of the physical properties of these systems has been concentrated on the search for flat band ferromagnetism[3,19,20], and also the analysis of their ground states in exact terms has been started[21].

Following the interest in increase in the number of lattice sites in the ring which forms the basis of the periodic chain, one arrives at chains of hexagons which are the subject of this paper. The hexagon chains are of real interest since are relatively abundant in nature. The main representative of the zig-zag hexagon chains at the level of organic materials, are the polyacenes. Acenes, or polyacenes are a class of polycyclic aromatic hydrocarbons made up of linearly fused hexagon rings. These systems attracted attention because of optoelectronic and electrical engineering application possibilities which have led even to organic field effect transistors in which pentacene is incorporated[4]. Furthermore, such chains present potential possibilities for the design of soluble acene-based transistors and circuits[5], tetracene and pentacene have been used for the design of light emitting devices[22], etc. Due to these properties, the polyacene structures have been studied extensively; the theoretical studies have been mostly confined to mean-field type of descriptions[23]. One notes that the interest in hexagonal chains and structures is not restricted exclusively to carbon based materials, since also other compounds present similar cell structure, for example boron-nitride ionic honeycomb systems[24], etc.

B. The aim and technique used

Recently, based on first principle calculations, the Coulomb interaction has been analyzed in acenes between two particles. It was shown[25] that the average Coulomb repulsion in these systems can reach values around $U_{eff} \sim 4 - 5eV$, the ratio of U_{eff} to the bandwidth W

being of order $U_{eff}/W \sim 2.3 - 7.6$. These results show that correlation effects are very prominent in this type of chains, leading the authors to the conjecture that by increasing the concentration of carriers in these systems, the Coulomb repulsion is expected to stabilize correlated magnetic ground states.

The present paper has the aim to analyze this conjecture at a genuine many-body level. In order to treat the correlations properly and create premises for valuable conclusions, the study is made here at exact level.

Exact results for the chains under consideration, taking into account their quasi 1D character and non-integrable nature, are extremely rare. One only knows exact ground states for triangle[9], and rhombus[8] cases. The method used allows the exact ground state to be deduced under general circumstances independent on dimensionality or integrability and it is based on a technique which uses positive semidefinite operator characteristics. A positive semidefinite operator $\hat{P}$, is the operator which has the property $\langle\phi|\hat{P}|\phi\rangle \geq 0$ for all vectors $|\phi\rangle$ of the Hilbert space $\mathcal{H}$. It results that all eigenvalues p_i of $\hat{P}$, $\hat{P}|\phi_i\rangle = p_i|\phi_i\rangle$, are non-negative, e.g. $p_i \geq 0$. Consequently, if one succeeds in finding an exact decomposition of the Hamiltonian $\hat{H}$ in terms of positive semidefinite terms, namely $\hat{H} = \sum_n^m \hat{P}_n + C$, where $\hat{P}_n$ are positive semidefinite operators (whose number is m), and C is a constant depending on Hamiltonian parameters, then the operator $\hat{H}' = \hat{H} - C$ has a positive semidefinite form. Hence, $\hat{H}'$ has a spectrum bounded below by a well defined and known number, namely zero. As a result, the exact ground state of $\hat{H}'$ (consequently, also of $\hat{H}$), is given by the vector $|\Psi_g\rangle$ holding the property $\hat{H}'|\Psi_g\rangle = 0$, i.e. $\hat{P}_n|\Psi_g\rangle = 0$ must be satisfied for all $n = 1, 2, ..., m$.

The technique which we used is based on the above presented properties. First one has finds an exact decomposition of the Hamiltonian of the system in a positive semidefinite form, and obtain the explicit form of the positive semidefinite operators $\hat{P}_n$ for all n. In the second step one constructs the $|\Psi_g\rangle$ ground state Hilbert space vector such to satisfy $\hat{P}_n|\Psi_g\rangle = 0$ for all n. This procedure depends on the explicit form of the $\hat{P}_n$ operators, but one exemplifies below a particular case which will be used for the study of the zig-zag hexagon chain described below.

Let us assume that one has for $n = 1, 2, ...m_1 < m$ the structure $\hat{P}_n = \hat{A}_n^\dagger \hat{A}_n$ for the positive semidefinite operators $\hat{P}_n$, $n \leq m_1$, where $\hat{A}_n$ are built up from a linear combination of annihilation fermionic operators. In these conditions the construction of the ground state

starts by the construction of the wave vector $|\Psi\rangle = \prod_\mu \hat{B}_\mu^\dagger |0\rangle$ where $|0\rangle$ is the bare vacuum. The $\hat{B}_\mu^\dagger$ operators (constructed from fermionic creation operators), are objects which have to be deduced. Their calculation is made based on the anti-commutation relation $\{\hat{A}_n, \hat{B}_\mu^\dagger\} = 0$, which must be satisfied for all values of all indices n and μ. Indeed, if this anti-commutation relation holds, in $\hat{P}_n|\Psi\rangle = \hat{A}_n^\dagger \hat{A}_n (\prod_\mu \hat{B}_\mu^\dagger)|0\rangle$, the $\hat{A}_n$ operator can be pushed in front of the vacuum state obtaining $\hat{P}_n|\Psi\rangle = e^{i\phi}\hat{A}_n^\dagger (\prod_\mu \hat{B}_\mu^\dagger)\hat{A}_n|0\rangle$, which, given by the annihilation nature of $\hat{A}_n$ provides $\hat{A}_n|0\rangle = 0$. Consequently indeed $\hat{P}_n|\Psi\rangle = 0$ holds. The phase factor $e^{i\phi}$ provides only a $+1$, or -1 multiplicative factor depending on the even, or odd number of operators in $(\prod_\mu \hat{B}_\mu^\dagger)$.

After deducing all possible $\hat{B}_\mu^\dagger$ operators, the ground state $|\Psi_g\rangle$ is obtained by restricting the index $\mu \in I$, such to obtain $|\Psi_g\rangle = [\prod_{\mu \in I} \hat{B}_\mu^\dagger]|0\rangle$ based on the condition $\hat{P}_n|\Psi_g\rangle = 0$ also for $n > m_1$. The corresponding ground state energy becomes $E_g = C$. The carrier concentration at which $|\Psi_g\rangle$ is defined, is provided by the number of electrons introduced into the system by the $(\prod_{\mu \in I} \hat{B}_\mu^\dagger)$ operator product acting on the vacuum state $|0\rangle$.

One further notes that the transformation of the starting Hamiltonian $\hat{H}$ in a positive semidefinite form $\sum_n^m \hat{P}_n + C$ is not unique, can be performed in several different ways, each transformation places the final result in different regions of the parameter space. The parameter space domain in which the deduced ground state is present, is fixed by the matching conditions. These last are relations between the $\hat{H}$ parameters and the $\hat{P}_n$ parameters which allow the transcription of the starting $\hat{H}$ in the used positive semidefinite form.

The detailed presentation of the technique can be found in several recent publications[8,9,26,27]. The implementation of this method at finite value of the interaction has been started at the end of nineties[28,29,30,31,32,33] and has proven to be a successful and powerful technique leading to exact results even in situations unexpected in the context of exact solutions as: three dimensions[26,27], disordered and interacting systems in 2D[34], emergence of condensates[35,36], stripes and checkerboards in 2D[37], or insulator to metal transition driven by the Hubbard repulsion in 2D in vicinity of half filling[38]. We further note that similar techniques are used for spin models as well[39].

C. Overview of the obtained results

One analyzes the problem by concentrating on a fixed and given hexagon chain of zig-zag type (see Fig.1). The zig-zag nature must be accentuated since hexagon cells can be connected in a chain also in another way, namely in armchair configuration. The starting Hamiltonian, besides several hopping matrix elements and on-site one-particle potentials contains also the Coulomb repulsion as interaction, but for simplicity only at on-site level, providing the Hubbard interaction term with $U > 0$ strength. Since we are interested in finding valuable information about electron correlation effects in a fixed confined system, one keeps the chain structure unchanged during the study, e.g. phononic contributions are neglected. Since Peierls transitions caused by electron-phonon interactions in chain structures with even number of sites per cell could influence the emerging phases only around half-filling[19,20], one does not expect that the neglected phononic contributions will provide genuine changes in our results relating far from half-filling regions.

The Hamiltonian of the starting chain is transformed first in a positive semidefinite form. This transformation is important not only in the context of acene structures. This is because several other systems of large interest today are built up from hexagons. For example graphene, being a 2D hexagon structure constructed from the same cell, can be described at the level of the transformation into a positive semidefinite form by the same block operators as used here for the zig-zag hexagon chain in Section IV. The block operators applied for the transformation were such chosen to provide a not severely restricted phase diagram region where the conclusions are valid.

After this transformation one analyzes the bare band structure and one shows that flat bands are not possible to emerge. Hence, flat band ferromagnetism[13,14] (often studied in the context of conducting chains, see for example[3,19,20]) is excluded *a priori* from the spectrum of possible magnetic phases.

After the positive semidefinite form of the Hamiltonian has been obtained, one turns to the construction of the ground states $|\Psi_g\rangle$. This step starts with the deduction of the operators denoted hereafter by $\hat{B}_\mu^\dagger$, building up $|\Psi_g\rangle$. One notes that the label index μ has also a spin component. Interestingly, it turns out that all these operators are extended, i.e. have components placed in each cell and cannot be introduced in a restricted domain of the chain with extension smaller than the system size in the direction of the primitive vector.

The extended nature of all $\hat{B}_{\mu}^{\dagger}$ operators is a special characteristic of the hexagon chains, which has not been observed previously in the case of triangle, quadrilateral and pentagon chains[8,9,21]. This aspect is important for two reasons. First, the methods for the treatment and deduction of the extended operators in the context of the positive semidefinite operator technique are practically completely open and unknown. On this line one notes that even if it has been shown that the treatment in another context of the extended operators is feasible[40], one has only one case described quite recently in the literature, namely in the study of the insulator to metal transition driven by the Hubbard repulsion in 2D in the vicinity of half filling[38]. Since a strategy developed for 2D, directly cannot be applied for quasi 1D structures, at this point a special technique has been constructed and described for the deduction of the $\hat{B}_{\mu}^{\dagger}$ operators, which can be used for other chain structures as well. Second, the extended nature of $\hat{B}_{\mu}^{\dagger}$ terms is present in a confined space region delimited by the chain itself. Consequently, by increasing the carrier concentration (i.e. increasing the number of independent $\hat{B}_{\mu}^{\dagger}$ operators in $|\Psi_g\rangle$), the $\hat{B}_{\mu}^{\dagger}$ operators present in the ground state wave vector will satisfy connectivity conditions (i.e. will act on common lattice sites). Given by this, the spin indices of the electrons must be correlated in order to avoid as much as possible the double occupancy and to reduce in this manner the ground state energy. This is the route for the emergence of ferromagnetism in these systems. The obtained results show that the conjecture by Brocks et al.[25] made at two-particle level for acenes is indeed viable in a rigorous many-body frame provided by a fixed zig-zag hexagon chain described by a Hubbard type of model.

The remaining part of the paper is structured as follows: Section II. describes in detail the system of interest and its Hamiltonian, Section III. analyzes the non-interacting band structure, Section IV. presents the transformation of the Hamiltonian in a positive semidefinite form, Section V. solves the matching conditions, Section VI. presents the deduction strategy for the exact ground states, and the obtained ground states together with their physical properties, and Section VII. containing the summary and conclusions closes the presentation. The Appendix contains mathematical details related to the exemplification in a simple case of the deduced ground states.

II. THE SYSTEM OF INTEREST

The zig-zag hexagon chain is presented in Fig.1. In the cell constructed at the site $\mathbf{i}$ one has 4 lattice sites whose position relative to the site $\mathbf{i}$ is given by the vectors $\mathbf{r}_\nu$, $\nu = 1, 2, 3, 4$. The system contains four sublattices S_ν containing the lattice sites $\mathbf{i}+\mathbf{r}_\nu \in S_\nu$, hence ν represents as well the sublattice index. For mathematical simplicity one considers $\mathbf{r}_1 = 0$ during the calculations. The primitive Bravais vector $\mathbf{a}$ is directed along the line of the chain. The hexagon side is $b = a/\sqrt{3}$, where $a = |\mathbf{a}|$ is the lattice constant. One considers below a chain build up from N_c cells, the number of lattice sites being $N_\Lambda = 4N_c$, while the number of electrons is denoted by N.

The Hamiltonian of the system $\hat{H} = \hat{H}_0 + \hat{H}_U$ is given by

$$\begin{aligned}
\hat{H}_0 &= \sum_\sigma \sum_{\mathbf{i}=1}^{N_c} \{ [t(\hat{c}^\dagger_{\mathbf{i}+\mathbf{r}_2,\sigma}\hat{c}_{\mathbf{i}+\mathbf{r}_1,\sigma} + \hat{c}^\dagger_{\mathbf{i}+\mathbf{r}_1+\mathbf{a},\sigma}\hat{c}_{\mathbf{i}+\mathbf{r}_2,\sigma} + \hat{c}^\dagger_{\mathbf{i}+\mathbf{r}_4,\sigma}\hat{c}_{\mathbf{i}+\mathbf{r}_3+\mathbf{a},\sigma} + \hat{c}^\dagger_{\mathbf{i}+\mathbf{r}_3,\sigma}\hat{c}_{\mathbf{i}+\mathbf{r}_4,\sigma}) \\
&+ t_1\hat{c}^\dagger_{\mathbf{i}+\mathbf{r}_1,\sigma}\hat{c}_{\mathbf{i}+\mathbf{r}_3,\sigma} + H.c.] + [t'(\hat{c}^\dagger_{\mathbf{i}+\mathbf{r}_2,\sigma}\hat{c}_{\mathbf{i}+\mathbf{r}_3,\sigma} + \hat{c}^\dagger_{\mathbf{i}+\mathbf{r}_3+\mathbf{a},\sigma}\hat{c}_{\mathbf{i}+\mathbf{r}_2,\sigma} + \hat{c}^\dagger_{\mathbf{i}+\mathbf{r}_4,\sigma}\hat{c}_{\mathbf{i}+\mathbf{r}_1+\mathbf{a},\sigma} \\
&+ \hat{c}^\dagger_{\mathbf{i}+\mathbf{r}_1,\sigma}\hat{c}_{\mathbf{i}+\mathbf{r}_4,\sigma}) + t'_1(\hat{c}^\dagger_{\mathbf{i}+\mathbf{r}_1+\mathbf{a},\sigma}\hat{c}_{\mathbf{i}+\mathbf{r}_1,\sigma} + \hat{c}^\dagger_{\mathbf{i}+\mathbf{r}_3+\mathbf{a},\sigma}\hat{c}_{\mathbf{i}+\mathbf{r}_3,\sigma}) \\
&+ t_e(\hat{c}^\dagger_{\mathbf{i}+\mathbf{r}_2+\mathbf{a},\sigma}\hat{c}_{\mathbf{i}+\mathbf{r}_2,\sigma} + \hat{c}^\dagger_{\mathbf{i}+\mathbf{r}_4+\mathbf{a},\sigma}\hat{c}_{\mathbf{i}+\mathbf{r}_4,\sigma}) + H.c.] \\
&+ [\epsilon_0(\hat{n}_{\mathbf{i}+\mathbf{r}_2,\sigma} + \hat{n}_{\mathbf{i}+\mathbf{r}_4,\sigma}) + \epsilon_1(\hat{n}_{\mathbf{i}+\mathbf{r}_1,\sigma} + \hat{n}_{\mathbf{i}+\mathbf{r}_3,\sigma})], \\
\hat{H}_U &= U\sum_{\mathbf{i}=1}^{N_c}\sum_{\nu=1}^{4} \hat{n}_{\mathbf{i}+\mathbf{r}_\nu,\uparrow}\hat{n}_{\mathbf{i}+\mathbf{r}_\nu,\downarrow},
\end{aligned} \tag{1}$$

where $\hat{c}^\dagger_{\mathbf{j},\sigma}$ is the canonical Fermi operator creating an electron at the site $\mathbf{j}$ with spin projection σ, and $\hat{n}_{\mathbf{i},\sigma} = \hat{c}^\dagger_{\mathbf{i},\sigma}\hat{c}_{\mathbf{i},\sigma}$ represents the particle number operator for electrons with spin σ placed at the lattice site $\mathbf{i}$. Since real systems are in view, several hopping matrix elements are considered in (1). The t and t_1 terms characterize nearest neighbor hopping matrix elements (t_1 is placed perpendicular to the line of the chain). The t', t'_1, t_e contributions represent next nearest neighbor hopping matrix elements (t'_1 and t_e are directed along the line of the chain, t'_1 connects internal sites while t_e external sites of the chain). The ϵ_0, ϵ_1 parameters are on-site one-particle potentials (ϵ_0 is placed on external sites), see Fig.2. Finally, $\hat{H}_U$ characterizes the on-site Coulomb repulsion where $U > 0$ is considered.

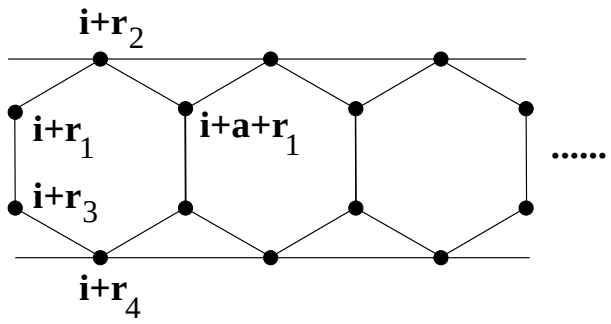

FIG. 1: The studied zig-zag hexagon chain. The cell constructed at the site **i** contains 4 sites whose in-cell positions relative to **i** are specified by the vectors $\mathbf{r}_\nu$, $\nu = 1, 2, 3, 4$, where, for convenience one takes $\mathbf{r}_1 = 0$. The vector **a** represents the unique primitive vector of the Bravais lattice. In the same time, $\mathbf{r}_\nu$ denotes lattice sites in four different sublattices S_ν.

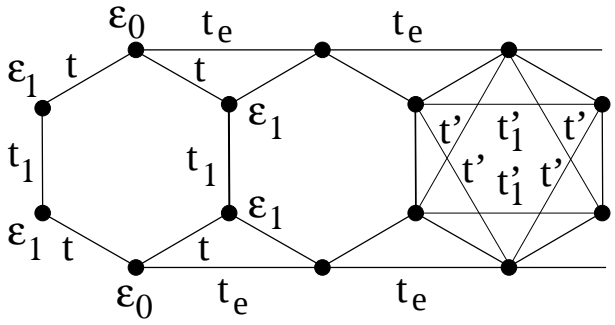

FIG. 2: The parameters of the kinetic part of the Hamiltonian. The t and t_1 terms represent nearest neighbor hopping matrix elements from which t_1 is placed along the touching bonds between hexagons. t', t'_1 and t_e are hopping matrix elements describing next nearest neighbor hoppings. From these t_e describes the external hopping relative to hexagons, while t'_1 is parallel to the line of the chain, being placed inside the hexagons. Finally, ϵ_1, (ϵ_0) represents the on-site potential on contact points between hexagons (external sites of hexagons). For the clarity of the notations, the next nearest neighbor hoppings are separately presented in the third cell of the figure.

III. THE NON-INTERACTING BAND STRUCTURE

A. The deduction of the bare band structure

In order to deduce the non-interacting band structure one transforms $\hat{H}_0$ from (1) in $\mathbf{k}$-space. For this one Fourier transforms the $\hat{c}_{\mathbf{j},\sigma}$ operators as follows

$$\hat{c}_{\mathbf{i}+\mathbf{r}_\nu+\mathbf{r},\sigma} = \frac{1}{\sqrt{N_c}} \sum_{\mathbf{k}=1}^{N_c} \hat{c}_{\nu,\mathbf{k},\sigma} e^{-i\mathbf{k}(\mathbf{i}+\mathbf{r}_\nu+\mathbf{r})}, \tag{2}$$

where $\hat{c}_{\nu,\mathbf{k},\sigma}$ represents the annihilation operator for the state $(\mathbf{k},\sigma)$ in the sublattice ν. Note that one has $\mathbf{r}_1 = 0$, and $\mathbf{r}$ from (2) takes two possible values, namely 0 and $\mathbf{a}$. Substituting (2) in (1), one finds

$$\begin{aligned}
\hat{H}_0 \;=\; & \sum_{\sigma} \sum_{\mathbf{k}} \{ [t_{1,2}(\mathbf{k}) \hat{c}^{\dagger}_{1,\mathbf{k},\sigma} \hat{c}_{2,\mathbf{k},\sigma} + t_{1,3}(\mathbf{k}) \hat{c}^{\dagger}_{1,\mathbf{k},\sigma} \hat{c}_{3,\mathbf{k},\sigma} + t_{3,4}(\mathbf{k}) \hat{c}^{\dagger}_{3,\mathbf{k},\sigma} \hat{c}_{4,\mathbf{k},\sigma} + H.c.] \\
& + \; [t_{1,4}(\mathbf{k}) \hat{c}^{\dagger}_{1,\mathbf{k},\sigma} \hat{c}_{4,\mathbf{k},\sigma} + t_{2,3}(\mathbf{k}) \hat{c}^{\dagger}_{2,\mathbf{k},\sigma} \hat{c}_{3,\mathbf{k},\sigma} + t_{1,1}(\mathbf{k}) \hat{c}^{\dagger}_{1,\mathbf{k},\sigma} \hat{c}_{1,\mathbf{k},\sigma} \\
& + \; t_{2,2}(\mathbf{k}) \hat{c}^{\dagger}_{2,\mathbf{k},\sigma} \hat{c}_{2,\mathbf{k},\sigma} + t_{3,3}(\mathbf{k}) \hat{c}^{\dagger}_{3,\mathbf{k},\sigma} \hat{c}_{3,\mathbf{k},\sigma} + t_{4,4}(\mathbf{k}) \hat{c}^{\dagger}_{4,\mathbf{k},\sigma} \hat{c}_{4,\mathbf{k},\sigma} + H.c.] \\
& + \; [\epsilon_0 (\hat{c}^{\dagger}_{2,\mathbf{k},\sigma} \hat{c}_{2,\mathbf{k},\sigma} + \hat{c}^{\dagger}_{4,\mathbf{k},\sigma} \hat{c}_{4,\mathbf{k},\sigma}) + \epsilon_1 (\hat{c}^{\dagger}_{1,\mathbf{k},\sigma} \hat{c}_{1,\mathbf{k},\sigma} + \hat{c}^{\dagger}_{3,\mathbf{k},\sigma} \hat{c}_{3,\mathbf{k},\sigma})] \},
\end{aligned} \tag{3}$$

where the first, second and third, and fourth rows represent in order the nearest neighbor, next nearest neighbor, and on-site contributions. Furthermore one has

$$\begin{aligned}
& t_{1,2}(\mathbf{k}) = t(e^{+i\mathbf{k}(\mathbf{a}-\mathbf{r}_2)} + e^{-i\mathbf{k}\mathbf{r}_2}), \quad t_{1,3}(\mathbf{k}) = t_1 e^{-i\mathbf{k}\mathbf{r}_3}, \quad t_{3,4}(\mathbf{k}) = t(e^{+i\mathbf{k}(\mathbf{r}_3-\mathbf{r}_4)} + e^{-i\mathbf{k}(\mathbf{r}_4-\mathbf{r}_3-\mathbf{a})}), \\
& t_{1,4}(\mathbf{k}) = t'(e^{-i\mathbf{k}\mathbf{r}_4} + e^{-i\mathbf{k}(\mathbf{r}_4-\mathbf{a})}), \quad t_{2,3}(\mathbf{k}) = t'(e^{+i\mathbf{k}(\mathbf{r}_2-\mathbf{r}_3)} + e^{-i\mathbf{k}(\mathbf{r}_3+\mathbf{a}-\mathbf{r}_2)}), \\
& t_{1,1}(\mathbf{k}) = t'_1 e^{+i\mathbf{k}\mathbf{a}}, \quad t_{2,2}(\mathbf{k}) = t_e e^{+i\mathbf{k}\mathbf{a}}, \quad t_{3,3}(\mathbf{k}) = t'_1 e^{+i\mathbf{k}\mathbf{a}}, \quad t_{4,4}(\mathbf{k}) = t_e e^{+i\mathbf{k}\mathbf{a}},
\end{aligned} \tag{4}$$

where for $\mathbf{r}_\nu$, $\nu = 2,3,4$, see Fig.1, while $\mathbf{a}$ represents the primitive vector of the Bravais lattice. Taking into consideration a Cartesian system of coordinates with versors $(\mathbf{i}_1, \mathbf{j}_1)$ whose x-axis is directed along the line of the chain, one has

$$\mathbf{r}_1 = 0, \quad \mathbf{r}_2 = \frac{a}{2}\mathbf{i}_1 + \frac{a}{2\sqrt{3}}\mathbf{j}_1, \quad \mathbf{r}_3 = -\frac{a}{\sqrt{3}}\mathbf{j}_1, \quad \mathbf{r}_4 = \frac{a}{2}\mathbf{i}_1 - \frac{a\sqrt{3}}{2}\mathbf{j}_1, \tag{5}$$

where $a = |\mathbf{a}|$ holds.

Introducing the 1×4 row vector $\mathbf{C}^{\dagger}$ and its 4×1 adjoint $\mathbf{C}$ by

$$\mathbf{C}^{\dagger} = (\hat{c}^{\dagger}_{1,\mathbf{k},\sigma}, \hat{c}^{\dagger}_{2,\mathbf{k},\sigma}, \hat{c}^{\dagger}_{3,\mathbf{k},\sigma}, \hat{c}^{\dagger}_{4,\mathbf{k},\sigma}), \qquad \mathbf{C} = \begin{pmatrix} \hat{c}_{1,\mathbf{k},\sigma} \\ \hat{c}_{2,\mathbf{k},\sigma} \\ \hat{c}_{3,\mathbf{k},\sigma} \\ \hat{c}_{4,\mathbf{k},\sigma} \end{pmatrix}, \tag{6}$$

one observes that (3) can be written in a matrix product form, namely

$$\hat{H}_0 = \sum_{\sigma} \sum_{\mathbf{k}} \mathbf{C}^{\dagger} \tilde{\mathbf{M}} \mathbf{C}, \tag{7}$$

where, introducing the notation $f(\mathbf{k}) = (1 + e^{+i\mathbf{ka}})$, for the matrix $\tilde{\mathbf{M}}$ one has

$$\tilde{\mathbf{M}} = \begin{pmatrix} \epsilon_1 + 2t_1' \cos \mathbf{ak} & te^{-i\mathbf{kr}_2} f(\mathbf{k}) & t_1 e^{-i\mathbf{kr}_3} & t' e^{-i\mathbf{kr}_4} f(\mathbf{k}) \\ te^{+i\mathbf{kr}_2} f^*(\mathbf{k}) & \epsilon_0 + 2t_e \cos \mathbf{ak} & t' e^{-i\mathbf{k}(\mathbf{r}_3 - \mathbf{r}_2)} f^*(\mathbf{k}) & 0 \\ t_1 e^{+i\mathbf{kr}_3} & t' e^{+i\mathbf{k}(\mathbf{r}_3 - \mathbf{r}_2)} f(\mathbf{k}) & \epsilon_1 + 2t_1' \cos \mathbf{ak} & te^{-i\mathbf{k}(\mathbf{r}_4 - \mathbf{r}_3)} f(\mathbf{k}) \\ t' e^{+i\mathbf{kr}_4} f^*(\mathbf{k}) & 0 & te^{+i\mathbf{k}(\mathbf{r}_4 - \mathbf{r}_3)} f^*(\mathbf{k}) & \epsilon_0 + 2t_e \cos \mathbf{ak} \end{pmatrix}. \tag{8}$$

The bare band structure is obtained from the secular equation of the matrix $\tilde{\mathbf{M}}$ from (8) which provides

$$\begin{aligned} &(\epsilon_0 - \lambda + 2t_e \cos \mathbf{ak})^2 [(\epsilon_1 - \lambda + 2t_1' \cos \mathbf{ak})^2 - t_1^2] + (\epsilon_0 - \lambda + 2t_e \cos \mathbf{ak}) |f(\mathbf{k})|^2 \\ &\times [2tt_1 t' - (\epsilon_1 - \lambda + 2t_1' \cos \mathbf{ak})(t'^2 + t^2)] - t|f(\mathbf{k})|^2 [t(\epsilon_0 - \lambda + 2t_e \cos \mathbf{ak})(\epsilon_1 - \lambda + 2t_1' \cos \mathbf{ak}) \\ &-(\epsilon_0 - \lambda + 2t_e \cos \mathbf{ak}) t' t_1 + |f(\mathbf{k})|^2 t(t'^2 - t^2)] - t'|f(\mathbf{k})|^2 [t'(\epsilon_0 - \lambda + 2t_e \cos \mathbf{ak}) \\ &\times (\epsilon_1 - \lambda + 2t_1' \cos \mathbf{ak}) - (\epsilon_0 - \lambda + 2t_e \cos \mathbf{ak}) tt_1 + |f(\mathbf{k})|^2 t'(t^2 - t'^2)] = 0. \end{aligned} \tag{9}$$

The non-interacting band structure containing 4 bands is obtained from the solutions $E_\eta(\mathbf{k}) = \lambda$ of the quadratic algebraic equation (9), which provides four solutions $\eta = 1, 2, 3, 4$. One further notes that in (9), $|f(\mathbf{k})|^2 = 2(1 + \cos \mathbf{ak})$ holds, and $k = \mathbf{ak} \in (-\pi, \pi]$ is satisfied for the first Brillouin zone.

Introducing the notation $\bar{\epsilon}_\alpha = \epsilon_\alpha - \lambda$ for $\alpha = 0, 1$, from (9) one obtains the equation for the bare band structure in the form

$$\begin{aligned} &(\bar{\epsilon}_0 + 2t_e \cos k)^2 [(\bar{\epsilon}_1 + 2t_1' \cos k)^2 - t_1^2] - 4(\bar{\epsilon}_0 + 2t_e \cos k)(1 + \cos k) \\ &\times [(\bar{\epsilon}_1 + 2t_1' \cos k)(t^2 + t'^2) - 2tt_1 t'] + 4(1 + \cos k)^2 (t'^2 - t^2)^2 = 0. \end{aligned} \tag{10}$$

B. The properties of the bare band structure

A picture representing an exemplification for the bare band structure is presented in Fig.3. Modifying the parameter values, one obtains cusp points which can be considered in a given extent reminiscent of the Dirac points present in the graphene case[41], see Fig.4. But

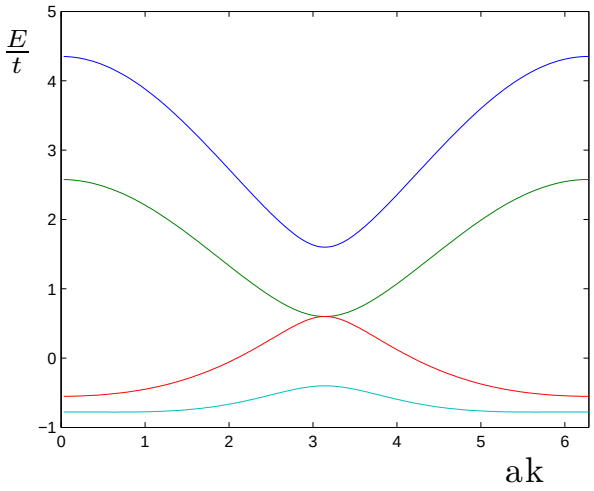

FIG. 3: An exemplifying image for the band structure plotted on a 2π domain for the k variable. The used parameters are $t_1/t = 1, t'/t = 0.2, t'_1/t = 0.2, t_e/t = 0.2, \epsilon_0/t = 1, \epsilon_1/t = 1$. By modifying the $\hat{H}_0$ parameter values and signs, the relative inter-band distances and band shapes can be changed.

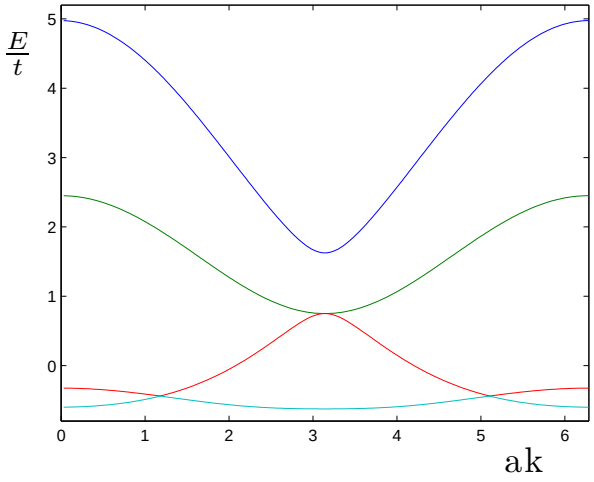

FIG. 4: Band structure with cusp points plotted at $t_1/t = 1.8/1.6, t'/t = 0.5/1.6, t'_1/t = 0.6/1.6, t_e/t = 0.2/1.6, \epsilon_0/t = 1, \epsilon_1/t = 2/1.6$ parameter values.

since in the studied case, the $|k \pm k^*|$ values not provide the same energy around the cusp points k^*, for small k, Dirac points in rigorous terms are not present here. Another case with closely situated intersection points for the lower two bands is presented in Fig.5.

It is important to underline that flat bands are not possible to occur for the studied

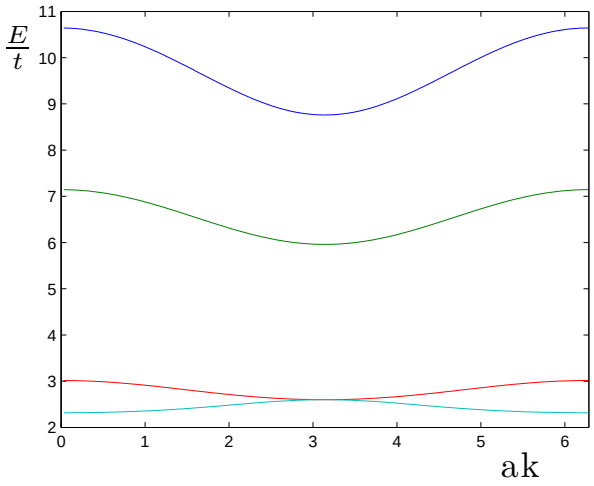

FIG. 5: Band structure with closely situated intersection points plotted at $t_1/t = 1.4, t'/t = 0.2, t_1'/t = 0.2, t_e/t = 0.2, \epsilon_0/t = 3, \epsilon_1/t = 7.76$ parameter values.

system. In order to show this one writes (10) into the form

$$A_4 \cos^4 k + A_3 \cos^3 k + A_2 \cos^2 k + A_1 \cos k + A_0 = 0, \tag{11}$$

where $A_n = A_n(\epsilon_0, \epsilon_1, t, t', t_1, t_1', t_e, \lambda)$ for all $n = 0, 1, ..., 4$ are k independent. Flat bands (e.g. k independences in λ) are obtained if simultaneously $A_n = 0$ holds for all n. This provides the following system of equations

$$\begin{aligned}
A_4(\epsilon_0, \epsilon_1, t, t_1, t', t_1', t_e, \lambda) &= 16 t_e^2 t_1'^2 \\
A_3(\epsilon_0, \epsilon_1, t, t_1, t', t_1', t_e, \lambda) &= 16(\epsilon_0 - \lambda) t_e t_1'^2 + 16(\epsilon_1 - \lambda) t_e^2 t_1' - 16 t_e t_1' (t^2 + t'^2) \\
A_2(\epsilon_0, \epsilon_1, t, t_1, t', t_1', t_e, \lambda) &= 4 t_1'^2 (\epsilon_0 - \lambda)^2 + 16(\epsilon_0 - \lambda)(\epsilon_1 - \lambda) t_e t_1' + 4 t_e^2 (\epsilon_1 - \lambda)^2 - 4 t_e^2 t_1^2 \\
&\quad -16 t_e t_1' (t^2 + t'^2) - 8 t_1' (\epsilon_0 - \lambda)(t^2 + t'^2) - 8 t_e (\epsilon_1 - \lambda)(t^2 + t'^2) + 16 t t_1 t' t_e + 4(t'^2 - t^2)^2 \\
A_1(\epsilon_0, \epsilon_1, t, t_1, t', t_1', t_e, \lambda) &= 4(\epsilon_0 - \lambda)^2 (\epsilon_1 - \lambda) t_1' + 4(\epsilon_0 - \lambda)(\epsilon_1 - \lambda)^2 t_e - 4 t_1^2 t_e (\epsilon_0 - \lambda) \\
&\quad -8 t_1' (\epsilon_0 - \lambda)(t^2 + t'^2) - 8 t_e (\epsilon_1 - \lambda)(t^2 + t'^2) - 4(\epsilon_0 - \lambda)(\epsilon_1 - \lambda)(t^2 + t'^2) \\
&\quad +8 t t_1 t' (\epsilon_0 - \lambda) + 16 t t_1 t' t_e + 8(t'^2 - t^2)^2 \\
A_0(\epsilon_0, \epsilon_1, t, t_1, t', t_1', t_e, \lambda) &= (\epsilon_0 - \lambda)^2 (\epsilon_1 - \lambda)^2 - t_1^2 (\epsilon_0 - \lambda)^2 - 4(\epsilon_0 - \lambda)(\epsilon_1 - \lambda)(t^2 + t'^2) \\
&\quad +8 t t_1 t' (\epsilon_0 - \lambda) + 4(t'^2 - t^2)^2.
\end{aligned} \tag{12}$$

As seen, (12) presents $A_n = 0$ solutions for all n only at $t_e t_1' = 0$, hence taking non-zero values for all introduced hopping terms, flat bands are not possible to occur into the system.

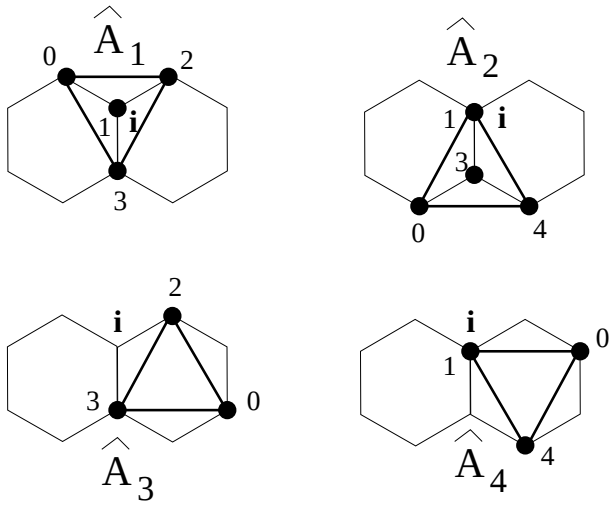

FIG. 6: The lattice sites on which the block operators $\hat{A}_{\nu,\mathbf{i},\sigma}$, $\nu = 1,2,3,4$ are defined for the cell constructed at the site $\mathbf{i}$. In each figure the position of the site $\mathbf{i}$ is explicitly shown. The numbers are representing the numbering of the coefficients of $\hat{A}_{\nu,\mathbf{i},\sigma}$ operators (see also (13)).

IV. THE TRANSFORMATION OF THE HAMILTONIAN IN POSITIVE SEMIDEFINITE FORM

One introduces four block operators $\hat{A}_{\nu,\mathbf{i},\sigma}$, $\nu = 1,2,3,4$ defined in the cell constructed at the site $\mathbf{i}$ by the following relations

$$\begin{aligned}
\hat{A}_{1,\mathbf{i},\sigma} &= a_1\hat{c}_{\mathbf{i}+\mathbf{r}_1,\sigma} + a_2\hat{c}_{\mathbf{i}+\mathbf{r}_2,\sigma} + a_3\hat{c}_{\mathbf{i}+\mathbf{r}_3,\sigma} + a_0\hat{c}_{\mathbf{i}-\mathbf{a}+\mathbf{r}_2,\sigma},\\
\hat{A}_{2,\mathbf{i},\sigma} &= b_1\hat{c}_{\mathbf{i}+\mathbf{r}_1,\sigma} + b_3\hat{c}_{\mathbf{i}+\mathbf{r}_3,\sigma} + b_4\hat{c}_{\mathbf{i}+\mathbf{r}_4,\sigma} + b_0\hat{c}_{\mathbf{i}-\mathbf{a}+\mathbf{r}_4,\sigma},\\
\hat{A}_{3,\mathbf{i},\sigma} &= d_2\hat{c}_{\mathbf{i}+\mathbf{r}_2,\sigma} + d_3\hat{c}_{\mathbf{i}+\mathbf{r}_3,\sigma} + d_0\hat{c}_{\mathbf{i}+\mathbf{a}+\mathbf{r}_3,\sigma},\\
\hat{A}_{4,\mathbf{i},\sigma} &= e_1\hat{c}_{\mathbf{i}+\mathbf{r}_1,\sigma} + e_4\hat{c}_{\mathbf{i}+\mathbf{r}_4,\sigma} + e_0\hat{c}_{\mathbf{i}+\mathbf{a}+\mathbf{r}_1,\sigma},
\end{aligned} \tag{13}$$

The lattice sites on which the operators $\hat{A}_{\nu,\mathbf{i},\sigma}$ are defined for the cell constructed at the site $\mathbf{i}$ are presented in Fig.6.

Using periodic boundary conditions and based on (13), the Hamiltonian of the problem transforms into a positive semidefinite form as follows

$$\hat{H} = \sum_{\mathbf{i}=1}^{N_c}\sum_{\sigma}\sum_{\nu=1}^{4}\hat{A}^{\dagger}_{\nu,\mathbf{i},\sigma}\hat{A}_{\nu,\mathbf{i},\sigma} + \hat{H}_U + K\hat{N}, \tag{14}$$

where $\hat{N}$ denotes the operator of the total number of particles. The relation (14) holds if

the following matching conditions are satisfied

$$
\begin{aligned}
& t = a_2^* a_1 = a_1^* a_0 = b_4^* b_3 = b_3^* b_0, \\
& t_e = a_2^* a_0 = b_4^* b_0, \\
& t_1 = a_3^* a_1 + b_3^* b_1, \\
& t' = a_2^* a_3 + d_2^* d_3 = a_3^* a_0 + d_0^* d_2 = b_4^* b_1 + e_4^* e_1 = b_1^* b_0 + e_0^* e_4, \\
& t_1' = e_0^* e_1 = d_0^* d_3, \\
& \epsilon_0 - K = |a_0|^2 + |a_2|^2 + |d_2|^2 = |b_0|^2 + |b_4|^2 + |e_4|^2, \\
& \epsilon_1 - K = |a_1|^2 + |e_0|^2 + |e_1|^2 + |b_1|^2 = |b_3|^2 + |d_0|^2 + |d_3|^2 + |a_3|^2. \qquad (15)
\end{aligned}
$$

The matching conditions (15) have been obtained by calculating $\sum_{\mathbf{i}=1}^{N_c} \sum_{\sigma} \sum_{\nu=1}^{4} \hat{A}_{\nu,\mathbf{i},\sigma}^{\dagger} \hat{A}_{\nu,\mathbf{i},\sigma}$ from (14) and equating the result term by term to the expression of $\hat{H}_0$ from (1).

V. DEDUCTION OF $\hat{A}_{\nu,\mathbf{i},\sigma}$ OPERATORS

In deducing the block operators defined in (13) one must calculate the prefactors $a_\alpha, b_\alpha, d_\alpha, e_\alpha$ present in equations (13). These are obtained by solving the matching conditions (15).

Solving the equations present in (15) one proceeds as follows. The first two rows of Eq.(15) provide solutions only for $t_e > 0$ and taking into account real hopping matrix elements, give

$$
\begin{aligned}
& |a_1| = |b_3| = \frac{t}{\sqrt{t_e}}, \\
& a_2 = a_0 = \frac{t}{a_1^*}, \quad b_4 = b_0 = \frac{t}{b_3^*}. \qquad (16)
\end{aligned}
$$

The fifth row of (15) provides

$$
e_0 = \frac{t_1'}{e_1^*}, \quad d_0 = \frac{t_1'}{d_3^*}, \qquad (17)
$$

and the remaining equations from (15) transform into the form

$$
\begin{aligned}
& t_1 = a_3^* a_1 + a_1^* b_1 e^{-i\phi_1^a}, \\
& t' = t\frac{a_3}{a_1} + d_2^* d_3 = t\frac{a_3}{a_1} + t_1'\frac{d_2^*}{d_3^*}, \\
& t' = t\frac{b_1}{b_3} + e_4^* e_1 = t\frac{b_1}{b_3} + t_1'\frac{e_4^*}{e_1^*}, \\
& \epsilon_0 - K = 2t_e + |d_2|^2 = 2t_e + |e_4|^2, \\
& \epsilon_1 - K = \frac{t^2}{t_e} + \frac{{t_1'}^2}{|e_1|^2} + |e_1|^2 + |b_1|^2 = \frac{t^2}{t_e} + \frac{{t_1'}^2}{|d_3|^2} + |d_3|^2 + |a_3|^2. \qquad (18)
\end{aligned}
$$

The second and third line of (18) arises from the fourth row of (15). For the first line of (18), given by $|a_1| = |b_3|$ in (16), one uses $b_3 = a_1 e^{i\phi_1^a}$. Now from the second and third line of (18), besides the condition $t_1' > 0$, one finds $|d_3| = |e_1| = \sqrt{t_1'}$. Consequently, the last two equations from (18) give $|d_2| = |e_4|$, and $|b_1| = |a_3|$. Using $b_1 = a_3 e^{i\phi_3^a}$ from the previous condition, the first equation of (18) becomes

$$t_1 = a_3^* a_1 + a_1^* a_3 e^{i(\phi_3^a - \phi_1^a)}, \tag{19}$$

which, because of the real nature of t_1 gives $\phi_3^a = \phi_1^a$, from where $t_1 = a_3^* a_1 + a_1^* a_3 = 2Re(a_1^* a_3)$, furthermore $b_1/b_3 = a_3/a_1$ arises. At this step one observes that in (13) each $\hat{A}_{\nu,\mathbf{i},\sigma}$ operator can be multiplied by an arbitrary phase factor without changing the expression of the transformed Hamiltonian (14). Consequently, by this multiplication relating $\hat{A}_{1,\mathbf{i},\sigma}$, the prefactor a_1 can be taken real, hence from the expression of t_1 the parameter a_3 must also be real. As a consequence, $t_1 = 2a_1 a_3$ holds, from where

$$a_3 = \frac{t_1}{2a_1} = \frac{t_1\sqrt{t_e}}{2t}, \quad a_1 = \frac{t}{\sqrt{t_e}}. \tag{20}$$

As a result, one finds that the coefficients a_α are given by

$$a_0 = \sqrt{t_e}, \quad a_1 = \frac{t}{\sqrt{t_e}}, \quad a_2 = \sqrt{t_e}, \quad a_3 = \frac{t_1\sqrt{t_e}}{2t}. \tag{21}$$

In what follows one concentrates on the b_α coefficients. Given by $b_1 = a_3 e^{i\phi_3^a}, b_3 = a_1 e^{i\phi_1^a}$ where a_1, a_3 are real and $\phi_1^a = \phi_3^a$, a multiplication by $e^{-i\phi_1^a}$ of $\hat{A}_{2,\mathbf{i},\sigma}$ from (13) provides real b_1 and b_3. Hence (16,21) together with $b_1/b_3 = a_3/a_1 = t_1 t_e/(2t^2)$ gives

$$b_0 = \sqrt{t_e}, \quad b_1 = \frac{t_1\sqrt{t_e}}{2t}, \quad b_3 = \frac{t}{\sqrt{t_e}}, \quad b_4 = \sqrt{t_e}. \tag{22}$$

At this moment one continues the calculation by deducing e_α and d_α. From the real value of t', taking into account the second and third expression of (18), one observes that by fixing d_3 (similarly e_1) to be real by multiplication by a phase factor, then d_2 (similarly e_4) also becomes real. Consequently $t' = (t_1 t_e)/(2t) + d_2\sqrt{t_1'} = (t_1 t_e)/(2t) + e_4\sqrt{t_1'}$ and $d_3 = e_1 = \sqrt{t_1'}$ together with Eq.(17) provides

$$\begin{aligned} &e_0 = \sqrt{t_1'}, \quad e_1 = \sqrt{t_1'}, \quad e_4 = \frac{2tt' - t_1 t_e}{2t\sqrt{t_1'}}, \\ &d_0 = \sqrt{t_1'}, \quad d_2 = \frac{2tt' - t_1 t_e}{2t\sqrt{t_1'}}, \quad d_3 = \sqrt{t_1'}. \end{aligned} \tag{23}$$

From the last two lines of (18) one further finds the K value

$$K = \epsilon_0 - 2t_e - \frac{(2tt' - t_1 t_e)^2}{4t^2 t_1'}, \tag{24}$$

and a condition which must be satisfied by the Hamiltonian parameters, namely

$$\epsilon_0 = \epsilon_1 + 2(t_e - t_1') - \frac{t^2}{t_e} - \frac{t_1^2 t_e}{4t^2} + \frac{(2tt' - t_1 t_e)^2}{4t^2 t_1'}. \tag{25}$$

The equality (25) represents the requirement for the on-site potential ϵ_0 necessary to be satisfied in order to find the expression for the transformed Hamiltonian (14) a valid relation. Besides (25), the parameter space region where the transformation from (1) to the positive semidefinite form (14) of the Hamiltonian is valid, is described by $t_e > 0, t_1' > 0$. In the presence of all these conditions, the bare band structure is exemplified by Fig.5.

Using the results presented in (21-23) one finds for the block operators introduced in (13) the explicit expressions

$$\begin{aligned}
\hat{A}_{1,\mathbf{i},\sigma} &= \sqrt{t_e}(\hat{c}_{\mathbf{i}+\mathbf{r}_2-\mathbf{a},\sigma} + \hat{c}_{\mathbf{i}+\mathbf{r}_2,\sigma}) + \frac{t}{\sqrt{t_e}}\hat{c}_{\mathbf{i}+\mathbf{r}_1,\sigma} + \frac{t_1\sqrt{t_e}}{2t}\hat{c}_{\mathbf{i}+\mathbf{r}_3,\sigma}, \\
\hat{A}_{2,\mathbf{i},\sigma} &= \sqrt{t_e}(\hat{c}_{\mathbf{i}+\mathbf{r}_4-\mathbf{a},\sigma} + \hat{c}_{\mathbf{i}+\mathbf{r}_4,\sigma}) + \frac{t}{\sqrt{t_e}}\hat{c}_{\mathbf{i}+\mathbf{r}_3,\sigma} + \frac{t_1\sqrt{t_e}}{2t}\hat{c}_{\mathbf{i}+\mathbf{r}_1,\sigma}, \\
\hat{A}_{3,\mathbf{i},\sigma} &= \sqrt{t_1'}(\hat{c}_{\mathbf{i}+\mathbf{r}_3,\sigma} + \hat{c}_{\mathbf{i}+\mathbf{r}_3+\mathbf{a},\sigma}) + \frac{2tt' - t_1 t_e}{2t\sqrt{t_1'}}\hat{c}_{\mathbf{i}+\mathbf{r}_2,\sigma}, \\
\hat{A}_{4,\mathbf{i},\sigma} &= \sqrt{t_1'}(\hat{c}_{\mathbf{i}+\mathbf{r}_1,\sigma} + \hat{c}_{\mathbf{i}+\mathbf{a}+\mathbf{r}_1,\sigma}) + \frac{2tt' - t_1 t_e}{2t\sqrt{t_1'}}\hat{c}_{\mathbf{i}+\mathbf{r}_4,\sigma}.
\end{aligned} \tag{26}$$

VI. THE DEDUCTION OF EXACT GROUND STATES

The ground states are deduced in two steps. i) First one looks for $\hat{B}_\mu^\dagger$ operators proper for the construction of the ground state by

$$|\Psi_g\rangle = \prod_{\mu \in I} \hat{B}_\mu^\dagger |0\rangle, \tag{27}$$

where $|0\rangle$ is the bare vacuum, I is a set of parameters μ, and the $\hat{B}_\mu^\dagger$ operators satisfy

$$\{\hat{A}_{\nu,\mathbf{i},\sigma}, \hat{B}_\mu^\dagger\} = 0, \tag{28}$$

for all values of all indices ν, μ, σ and $\mathbf{i}$. The motivation for this step is that given by the requirement (28), for the wave vector $|\Psi\rangle = \prod_\mu \hat{B}_\mu^\dagger |0\rangle$, one has the property

$$\sum_{\mathbf{i}=1}^{N_c} \sum_\sigma \sum_{\nu=1}^{4} \hat{A}_{\nu,\mathbf{i},\sigma}^\dagger \hat{A}_{\nu,\mathbf{i},\sigma} |\Psi\rangle = 0. \tag{29}$$

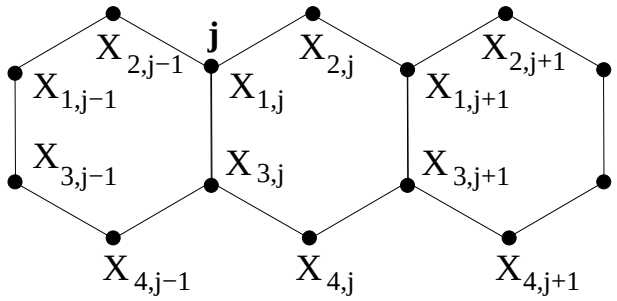

FIG. 7: The coefficients $x_{\nu,i}$ from (30) of the sites of the hexagon chain presented in the neighborhood of the lattice site $\mathbf{j}$.

Indeed, (29) holds since starting from (28), the $\hat{A}_{\nu,\mathbf{i},\sigma}$ operators in (29) can be pushed in front of the vacuum state, hence given by $\hat{A}_{\nu,\mathbf{i},\sigma}|0\rangle = 0$, the equality in Eq.(29) is satisfied.

In the second step ii) one chooses from all the possible $\hat{B}^{\dagger}_{\mu}$ operators those $\hat{B}^{\dagger}_{\mu_j}$, $I = \{\mu_1, \mu_2, ..., \mu_j, ..., \mu_M\}$, which satisfy also $\hat{H}_U(\prod_{\mu\in I}\hat{B}^{\dagger}_{\mu}|0\rangle) = 0$.

A. The operators needed for the construction of the ground state

1. Requirements for the operators building up the ground state

One considers the $\hat{B}^{\dagger}_{\mu}$ operators as the most general linear combination of creation operators with fixed spin projection acting on each lattice site of the system. Consequently, besides a fixed $\mu = \mu_1$ index, also the spin projection σ will be explicitly used as a label, and one has

$$\hat{B}^{\dagger}_{\mu_1,\sigma} = \sum_{\mathbf{j}} (x_{1,\mathbf{j}}\hat{c}^{\dagger}_{\mathbf{j}+\mathbf{r}_1,\sigma} + x_{2,\mathbf{j}}\hat{c}^{\dagger}_{\mathbf{j}+\mathbf{r}_2,\sigma} + x_{3,\mathbf{j}}\hat{c}^{\dagger}_{\mathbf{j}+\mathbf{r}_3,\sigma} + x_{4,\mathbf{j}}\hat{c}^{\dagger}_{\mathbf{j}+\mathbf{r}_4,\sigma}), \tag{30}$$

where the site $\mathbf{j}$ runs over all lattice sites of the sublattice S_1, and the $x_{\nu,i}$ coefficients represent the unknown variables which must be deduced. The placement of the coefficients $x_{\nu,i}$ is presented in Fig.7.

Now using (26,30) in (28), one finds the following linear equations for the $x_{\nu,i}$ coefficients

from (30) defined for the cell constructed at the site $\mathbf{i}=\mathbf{j}$

$$\begin{aligned}
&\sqrt{t_e}(x_{2,j}+x_{2,j-1})=-(\frac{t}{\sqrt{t_e}}x_{1,j}+\frac{t_1\sqrt{t_e}}{2t}x_{3,j}),\\
&\sqrt{t_e}(x_{4,j}+x_{4,j-1})=-(\frac{t_1\sqrt{t_e}}{2t}x_{1,j}+\frac{t}{\sqrt{t_e}}x_{3,j}),\\
&\sqrt{t_1'}(x_{1,j}+x_{1,j+1})=-Qx_{4,j},\\
&\sqrt{t_1'}(x_{3,j}+x_{3,j+1})=-Qx_{2,j},
\end{aligned}\tag{31}$$

where the notation $Q=(2tt'-t_1t_e)/(2t\sqrt{t_1'})$ has been introduced. From (31) one finds

$$\begin{aligned}
x_{1,j+1}&=(\frac{Qt_1}{2t\sqrt{t_1'}}-1)x_{1,j}+\frac{Qt}{t_e\sqrt{t_1'}}x_{3,j}+\frac{Q}{\sqrt{t_1'}}x_{4,j-1},\\
x_{3,j+1}&=(\frac{Qt_1}{2t\sqrt{t_1'}}-1)x_{3,j}+\frac{Qt}{t_e\sqrt{t_1'}}x_{1,j}+\frac{Q}{\sqrt{t_1'}}x_{2,j-1},\\
x_{2,j}&=-\frac{t}{t_e}x_{1,j}-\frac{t_1}{2t}x_{3,j}-x_{2,j-1},\\
x_{4,j}&=-\frac{t_1}{2t}x_{1,j}-\frac{t}{t_e}x_{3,j}-x_{4,j-1}.
\end{aligned}\tag{32}$$

The equations from (32) can be written in a matrix form as

$$\mathbf{Z}_j=\tilde{\mathbf{R}}\ \mathbf{Z}_{j-1},\tag{33}$$

where $\mathbf{Z}_j$ is a column vector with 4 components, which taken in order are given by $x_{1,j+1},x_{3,j+1},x_{2,j},x_{4,j}$. Similarly, $\mathbf{Z}_{j-1}$ is the column vector with elements $x_{1,j},x_{3,j},x_{2,j-1},x_{4,j-1}$

$$\mathbf{Z}_j=\begin{pmatrix}x_{1,j+1}\\x_{3,j+1}\\x_{2,j}\\x_{4,j}\end{pmatrix},\quad \mathbf{Z}_{j-1}=\begin{pmatrix}x_{1,j}\\x_{3,j}\\x_{2,j-1}\\x_{4,j-1}\end{pmatrix}.\tag{34}$$

Finally, the 4×4 matrix $\tilde{\mathbf{R}}$ is defined by

$$\tilde{\mathbf{R}}=\begin{pmatrix}\frac{Qt_1}{2t\sqrt{t_1'}}-1 & \frac{Qt}{t_e\sqrt{t_1'}} & 0 & \frac{Q}{\sqrt{t_1'}}\\ \frac{Qt}{t_e\sqrt{t_1'}} & \frac{Qt_1}{2t\sqrt{t_1'}}-1 & \frac{Q}{\sqrt{t_1'}} & 0\\ -\frac{t}{t_e} & -\frac{t_1}{2t} & -1 & 0\\ -\frac{t_1}{2t} & -\frac{t}{t_e} & 0 & -1\end{pmatrix}.\tag{35}$$

Starting from (35), in the following subsection one shows how it is possible to construct one (starting) $\hat{B}^{\dagger}_{\mu_1,\sigma}$ operator.

2. The construction of one starting $\hat{B}^{\dagger}_{\mu_1,\sigma}$ operator

Based on (33) one finds

$$\mathbf{Z}_{j+m} = \tilde{\mathbf{W}}_m \mathbf{Z}_j, \quad \tilde{\mathbf{W}}_m = (\tilde{\mathbf{R}})^m. \tag{36}$$

Consequently, since periodic boundary conditions are taken into account (i.e. after a finite number of m steps, in $\mathbf{Z}_{j+m}$ one must recovers $\mathbf{Z}_j$), an operator $\hat{B}^{\dagger}_{\mu_1,\sigma}$ from (30), proper for the construction of the ground state, is obtained when the matrix $\tilde{\mathbf{W}}_m$ has at least one eigenvalue 1. In this case the $x_{\alpha,i}$ unknown parameters from (30) are given exactly by the corresponding $\mathbf{Z}^e_j$ eigenvector

$$\tilde{\mathbf{W}}_m \mathbf{Z}^e_j = \mathbf{Z}^e_j. \tag{37}$$

One finds in this manner the starting coefficients $x_{\alpha,i}$ in the form

$$x_{1,j} = x^e_{1,j}, \quad x_{3,j} = x^e_{3,j}, \quad x_{2,j-1} = x^e_{2,j-1}, \quad x_{4,j-1} = x^e_{4,j-1}. \tag{38}$$

For the next $(m-1)$ cells $\mathbf{Z}_{j'}$, the coefficients $x_{1,j'}, x_{3,j'}, x_{2,j'-1}, x_{4,j'-1}$ are obtained by successive application of the $\tilde{\mathbf{R}}$ matrix to $\mathbf{Z}^e_j$ as follows: $x_{1,j+1}, x_{3,j+1}, x_{2,j}, x_{4,j}$ are obtained from $\mathbf{Z}_1$ deduced as $\mathbf{Z}_1 = \tilde{\mathbf{R}}\mathbf{Z}^e_j$; $x_{1,j+2}, x_{3,j+2}, x_{2,j+1}, x_{4,j+1}$ are obtained from $\mathbf{Z}_2$ deduced as $\mathbf{Z}_2 = (\tilde{\mathbf{R}})^2\mathbf{Z}^e_j$; etc.; $x_{1,j+m-1}, x_{3,j+m-1}, x_{2,j+m-2}, x_{4,j+m-2}$ are obtained from $\mathbf{Z}_{m-1}$ deduced as $\mathbf{Z}_{m-1} = (\tilde{\mathbf{R}})^{m-1}\mathbf{Z}^e_j$. Given by (37), for the coefficients $x_{1,j+m}, x_{3,j+m}, x_{2,j+m-1}, x_{4,j+m-1}$ entering in $\mathbf{Z}_m = (\tilde{\mathbf{R}})^m\mathbf{Z}^e_j$, the values $x_{1,j+m} = x_{1,j}, x_{3,j+m} = x_{3,j}, x_{2,j+m-1} = x_{2,j-1}, x_{4,j+m-1} = x_{4,j-1}$ are reobtained. After this step, starting from the coefficients $x_{1,j+m+1}, x_{3,j+m+1}, x_{2,j+m}, x_{4,j+m}$ present in $\mathbf{Z}_{m+1}$, the expressions are periodically repeated since $\mathbf{Z}_{m+1} = \tilde{\mathbf{R}}\mathbf{Z}^e_j$ holds again. In this manner a $\hat{B}^{\dagger}_{\mu_1,\sigma}$ operator has been constructed for a system characterized by $N_c = p \times m$, where p is an arbitrary positive integer.

3. Generation of new $\hat{B}^{\dagger}_{\mu_\alpha,\sigma}$ operators

Once a $\hat{B}^{\dagger}_{\mu_1,\sigma}$ operator has been deduced following the procedure described above, one has a proper operator for the construction of the ground state that has the obtained $x_{\alpha,i}$ coefficients structure holding a periodicity of m $\mathbf{Z}$ cells, the starting cell being the $\mathbf{j}$th cell $\mathbf{Z}_j$. If one moves the starting cell to the $\mathbf{Z}_{j+1}$ cell, one obtains a new, (usually) linearly

independent $\hat{B}^{\dagger}_{\mu_2,\sigma}$ operator. Repeating the procedure, starting from $\hat{B}^{\dagger}_{\mu_1,\sigma}$, maximum $(m-1)$ new operators $\hat{B}^{\dagger}_{\mu_\beta,\sigma}$, $\beta = 2,3,4,...,m$ can be created (the linear independence must be checked at each step). If more than one unity eigenvalues are present, the procedure can be repeated for each eigenvalue, constructing in this manner for the fixed m periodicity, maximum $q \times m$ different $\hat{B}^{\dagger}_{\mu,\sigma}$ operators, where q represents the number of unity eigenvalues corresponding to eigenvectors with non-zero norm. An exemplification is presented in the Appendix. The procedure can then be repeated for another m.

4. The ground state wave function

Using the operators deduced above, the $|\Psi\rangle$ wave vector described below (28) has the form

$$|\Psi\rangle = \prod_{\mu} \prod_{\sigma_\mu} \hat{B}^{\dagger}_{\mu,\sigma_\mu} |0\rangle. \tag{39}$$

One notes that the $\hat{B}^{\dagger}_{\mu,\sigma}$ operators (given by (33)) are all extended operators. Hence increasing the number of carriers and taking into account that all $\hat{B}^{\dagger}_{\mu,\sigma}$ operators are confined in the same quasi 1D structure, it results that connectivity conditions will be satisfied between different $\hat{B}^{\dagger}_{\mu,\sigma}$ operators with different μ indices (e.g. $\hat{B}^{\dagger}_{\mu_i,\sigma}$ and $\hat{B}^{\dagger}_{\mu_j,\sigma}$ operators for $i \neq j$ will touch each other, hence will act on a given finite number of common sites). For the example provided in the Appendix A. this happens starting from the $N = 2$ number of particles. Consequently, in order to minimize the ground state energy, all σ indices in (39) will be fixed to the same value ($\sigma_\mu = \sigma_{\mu'}$ for all μ, μ') providing in this manner zero double occupancy, hence a ferromagnetic ground state of the form

$$|\Psi_g\rangle = \prod_{\mu} \hat{B}^{\dagger}_{\mu,\sigma} |0\rangle, \tag{40}$$

where σ is fixed. Indeed $|\Psi_g\rangle$ from (40), as constructed from (39), will satisfy $(\sum_{\mathbf{i}=1}^{N_c} \sum_{\sigma} \sum_{\nu=1}^{4} \hat{A}^{\dagger}_{\nu,\mathbf{i},\sigma} \hat{A}_{\nu,\mathbf{i},\sigma}) |\Psi_g\rangle = 0$ for the first part of the transformed Hamiltonian from (14), while $\hat{H}_U |\Psi_g\rangle = 0$ will be given by the absence of the double occupancy. Consequently, $|\Psi_g\rangle$ represents the ground state of $\hat{H}$ from (14), the ground state energy being $E_g = KN$, where K is given in (24). Since one $\hat{B}^{\dagger}_{\mu,\sigma}$ operator introduces in fact one particle into the system, the particle number (hence the concentration of carriers) at which $|\Psi_g\rangle$ in (40) is defined, is given by the number of components of the product from (40).

As described, $|\Psi_g\rangle$ represents a ferromagnetic state. This ground state is itinerant and metallic because of the following reasons: i) the ground state wave function is extended, and ii) up to the N_{max} value equal to the number of components of the product from (40), one has for the particle number ($N < N_{max}$) dependent chemical potential μ_c, the expression $\delta\mu_c = \mu_c(+) - \mu_c(-) = 0$ where $\mu_c(+) = E_g(N+1) - E_g(N)$ and $\mu_c(-) = E_g(N) - E_g(N-1)$, see also Ref.[42].

Our up to date results show that the ferromagnetism emerges in the low concentration domain, a pedagogical example being presented in Appendix A. If one characterizes the carrier concentration by $n = N/N_c$ (i.e. average electron number per cell), the exemplified case in Appendix A. of six explicitly given operators describing through (40) six interacting electrons, even for a chain made of 36 cells (for example) gives $n = 1/6$, a far from zero finite concentration value. Consequently, the reported results clearly demonstrate the presence of itinerant ferromagnetism in the systems under study at low concentration, for finite chains (treated with periodic boundary conditions). Since 36 cells is a huge number for oligo-acenes (i.e. *few* linearly fused hexagons) placed in the center of the attention[25], our findings represent genuine information for potential application possibilities.

Furthermore, one underlines that since (as shown in Sec.III.) flat bands are not present in the system, the here described ferromagnetism is not of flat band type, and is provided by a joint effect of correlation and confinement.

One notes that for the finite sample case explicitly exemplified in Appendix A, the Hubbard repulsion must satisfy only the $U > 0$ condition, the U value itself being without importance. The phase diagram region where the presented solution occurs is not severely restricted. Besides two sign requirements present for two hopping matrix elements ($t_e, t_1' > 0$), only one condition for on-site one-particle potentials is present (see (25)), which requires a fixed value for ϵ_0 acting on external sites. Since this on-site potential can be tuned by an external gate potential[3], the described itinerant ferromagnetism can be in principle even switched on by an external electric field.

A detailed study of the phase diagram and the behavior in the thermodynamic limit is in preparation, and will be published elsewhere.

VII. SUMMARY AND CONCLUSIONS

A zig-zag hexagon chain described by a Hubbard type of model containing on-site Coulomb repulsion is analyzed in exact terms by a technique based on positive semidefinite operators. The calculations effectuated with periodic boundary conditions provide exact ground states of ferromagnetic and itinerant nature in the low concentration region. Flat bands are not present in the non-interacting band structure, and the ferromagnetism is created by a joint effect of correlations and confinement. The parameter space region where the described phase emerges is not severely restricted, and the unique on-site one-particle potential which must have a fixed value can in principle be tuned by external gate potentials.

The reason for the emergence of ferromagnetism is connected to two aspects. First, all operators entering in the construction of the ground state turn out to be extended. This is an interesting property of the studied system since it has not been observed for triangle, quadrilateral, and pentagon chains[8,9,21]. Second, all these extended operators with contributions in each cell act on lattice sites confined in the chain structure under consideration. Hence by increasing the carrier concentration, connectivity conditions between the operators of the ground state wave vector will emerge. These connectivity conditions (i.e. different operators describing different electrons act on common lattice sites) fix the spin indices to the same value, minimizing in this manner as much as possible the double occupancy in order to reduce the ground state energy, and provide the ferromagnetic ground state. The itinerant nature of the obtained ferromagnetic ground state may open new application possibilities in spintronics.

One adds below some observations related to the exact nature of the results. One knows that the flat band, or nearly flat band ferromagnetism can be described in exact terms[13,14]. Furthermore, it was shown that ferromagnetism emerging for completely dispersive band structure provided by spin-spin interactions in itinerant systems can also be described in exact terms[43]. The here reported results enlarge the spectrum of exact descriptions relating ferromagnetism in completely dispersive systems: one demonstrates that when the joint action of confinement and correlations is present, itinerant ferromagnetism can be described in exact terms at finite value of the interaction even in the frame of a non-extended Hubbard type of model.

The deduced results deserve a further observation as well: In the search for organic

ferromagnetism is no more necessary to look for hopping and on-site one-particle potential values in different chain structures in order to introduce flat bands in the system leading to flat band ferromagnetism. Itinerant ferromagnetism can be obtained even in completely dispersive systems, for example by a joint effect of correlations and confinement.

Acknowledgements

Z.G. gratefully acknowledges financial support provided by the Hungarian Research Fund through Contracts No. OTKA-T48782 and the Alexander von Humboldt Foundation.

APPENDIX A: EXEMPLIFICATION FOR THE CONSTRUCTION OF $\hat{B}^{\dagger}_{\mu,\sigma}$ OPERATORS

Let us consider the following pedagogical example for the construction of operators needed in the ground state wave vector. Using the notations $a = Q/\sqrt{t_1'}, b = t/t_e, c = t_1/(2t)$, the $\tilde{\mathbf{R}}$ matrix from (35) becomes

$$\tilde{\mathbf{R}} = \begin{pmatrix} ac-1 & ab & 0 & a \\ ab & ac-1 & a & 0 \\ -b & -c & -1 & 0 \\ -c & -b & 0 & -1 \end{pmatrix}. \tag{A1}$$

Using for simplicity the conditions $c = -b, a = -1/b$[44], for $\tilde{\mathbf{W}}_4$ one obtains four unity eigenvalues. One of eigenvectors has only zero elements (i.e. zero norm), so this cannot be used to construct physical states, but three other eigenvectors have non-zero norm. These are the following ones

$$\mathbf{Z}_1^e = \begin{pmatrix} 0 \\ 0 \\ -1 \\ 1 \end{pmatrix}, \quad \mathbf{Z}_2^e = \begin{pmatrix} 0 \\ 1 \\ 0 \\ 0 \end{pmatrix}, \quad \mathbf{Z}_3^e = \begin{pmatrix} 1 \\ 0 \\ 0 \\ 0 \end{pmatrix}. \tag{A2}$$

Let us consider first the $\mathbf{Z}_1^e$ eigenvector. For it one has

$$\tilde{\mathbf{R}}\mathbf{Z}_1^e = \begin{pmatrix} -\frac{1}{b} \\ \frac{1}{b} \\ 1 \\ -1 \end{pmatrix}, \quad \tilde{\mathbf{R}}^2\mathbf{Z}_1^e = \begin{pmatrix} 0 \\ 0 \\ 1 \\ -1 \end{pmatrix}, \quad \tilde{\mathbf{R}}^3\mathbf{Z}_1^e = \begin{pmatrix} \frac{1}{b} \\ -\frac{1}{b} \\ -1 \\ 1 \end{pmatrix}, \quad \tilde{\mathbf{R}}^4\mathbf{Z}_1^e = \begin{pmatrix} 0 \\ 0 \\ -1 \\ 1 \end{pmatrix}. \quad \text{(A3)}$$

Taking $\mathbf{Z}_j = \mathbf{Z}_1^e$ one finds based on (A3) the following starting $\hat{B}^\dagger_{\mu_1,\sigma}$ operator

$$\begin{aligned} \hat{B}^\dagger_{\mu_1,\sigma} \;=\; & ... + (-c^\dagger_{\mathbf{j}+\mathbf{r}_2,\sigma} + c^\dagger_{\mathbf{j}+\mathbf{r}_4,\sigma}) + (-\frac{1}{b}c^\dagger_{\mathbf{j}+2\mathbf{a}+\mathbf{r}_1,\sigma} + \frac{1}{b}c^\dagger_{\mathbf{j}+2\mathbf{a}+\mathbf{r}_3,\sigma} + c^\dagger_{\mathbf{j}+\mathbf{a}+\mathbf{r}_2,\sigma} - c^\dagger_{\mathbf{j}+\mathbf{a}+\mathbf{r}_4,\sigma}) \\ & + \; (c^\dagger_{\mathbf{j}+2\mathbf{a}+\mathbf{r}_2,\sigma} - c^\dagger_{\mathbf{j}+2\mathbf{a}+\mathbf{r}_4,\sigma}) + (\frac{1}{b}c^\dagger_{\mathbf{j}+4\mathbf{a}+\mathbf{r}_1,\sigma} - \frac{1}{b}c^\dagger_{\mathbf{j}+4\mathbf{a}+\mathbf{r}_3,\sigma} - c^\dagger_{\mathbf{j}+3\mathbf{a}+\mathbf{r}_2,\sigma} + c^\dagger_{\mathbf{j}+3\mathbf{a}+\mathbf{r}_4,\sigma}) \\ & + \; (-c^\dagger_{\mathbf{j}+4\mathbf{a}+\mathbf{r}_2,\sigma} + c^\dagger_{\mathbf{j}+4\mathbf{a}+\mathbf{r}_4,\sigma}) + ..., \end{aligned} \quad \text{(A4)}$$

where the contributions from fixed $\mathbf{Z}$ cells are collected in parentheses. The second $\hat{B}^\dagger_{\mu_2,\sigma}$ operator is obtained from (A4) by translating the starting point of the period with one cell, i.e. taking $\mathbf{Z}_{j+1} = \mathbf{Z}_1^e$. One gets

$$\begin{aligned} \hat{B}^\dagger_{\mu_2,\sigma} \;=\; & ... + (\frac{1}{b}c^\dagger_{\mathbf{j}+\mathbf{a}+\mathbf{r}_1,\sigma} - \frac{1}{b}c^\dagger_{\mathbf{j}+\mathbf{a}+\mathbf{r}_3,\sigma} - c^\dagger_{\mathbf{j}+\mathbf{r}_2,\sigma} + c^\dagger_{\mathbf{j}+\mathbf{r}_4,\sigma}) + (-c^\dagger_{\mathbf{j}+\mathbf{a}+\mathbf{r}_2,\sigma} + c^\dagger_{\mathbf{j}+\mathbf{a}+\mathbf{r}_4,\sigma}) \\ & + \; (-\frac{1}{b}c^\dagger_{\mathbf{j}+3\mathbf{a}+\mathbf{r}_1,\sigma} + \frac{1}{b}c^\dagger_{\mathbf{j}+3\mathbf{a}+\mathbf{r}_3,\sigma} + c^\dagger_{\mathbf{j}+2\mathbf{a}+\mathbf{r}_2,\sigma} - c^\dagger_{\mathbf{j}+2\mathbf{a}+\mathbf{r}_4,\sigma}) + (c^\dagger_{\mathbf{j}+3\mathbf{a}+\mathbf{r}_2,\sigma} - c^\dagger_{\mathbf{j}+3\mathbf{a}+\mathbf{r}_4,\sigma}) \\ & + \; (\frac{1}{b}c^\dagger_{\mathbf{j}+5\mathbf{a}+\mathbf{r}_1,\sigma} - \frac{1}{b}c^\dagger_{\mathbf{j}+5\mathbf{a}+\mathbf{r}_3,\sigma} - c^\dagger_{\mathbf{j}+4\mathbf{a}+\mathbf{r}_2,\sigma} + c^\dagger_{\mathbf{j}+4\mathbf{a}+\mathbf{r}_4,\sigma}) + ... \end{aligned} \quad \text{(A5)}$$

A further translation of $\mathbf{Z}_1^e$ to the following cell by taking $\mathbf{Z}_{j+2} = \mathbf{Z}_1^e$ provides $-\hat{B}^\dagger_{\mu_1,\sigma}$ while the fourth translation by taking $\mathbf{Z}_{j+3} = \mathbf{Z}_1^e$ reproduces $\hat{B}^\dagger_{\mu_1,\sigma}$. Hence these steps do not provide new linearly independent $\hat{B}^\dagger_{\mu,\sigma}$ operators.

Now one concentrates on the $\mathbf{Z}_2^e$ eigenvector. In this case one obtains

$$\tilde{\mathbf{R}}\mathbf{Z}_2^e = \begin{pmatrix} -1 \\ 0 \\ b \\ -b \end{pmatrix}, \quad \tilde{\mathbf{R}}^2\mathbf{Z}_2^e = \begin{pmatrix} 1 \\ 0 \\ 0 \\ 0 \end{pmatrix}, \quad \tilde{\mathbf{R}}^3\mathbf{Z}_2^e = \begin{pmatrix} 0 \\ -1 \\ -b \\ b \end{pmatrix}, \quad \tilde{\mathbf{R}}^4\mathbf{Z}_2^e = \begin{pmatrix} 0 \\ 1 \\ 0 \\ 0 \end{pmatrix}. \quad \text{(A6)}$$

Taking $\mathbf{Z}_j = \mathbf{Z}_2^e$ one obtains the third linearly independent $\hat{B}^\dagger_{\mu,\sigma}$ operator as follows

$$\begin{aligned} \hat{B}^\dagger_{\mu_3,\sigma} \;=\; & ... + (\hat{c}^\dagger_{\mathbf{j}+\mathbf{a}+\mathbf{r}_3,\sigma}) + (-\hat{c}^\dagger_{\mathbf{j}+2\mathbf{a}+\mathbf{r}_1,\sigma} + b\hat{c}^\dagger_{\mathbf{j}+\mathbf{a}+\mathbf{r}_2,\sigma} - b\hat{c}^\dagger_{\mathbf{j}+\mathbf{a}+\mathbf{r}_4,\sigma}) \\ & + \; (\hat{c}^\dagger_{\mathbf{j}+3\mathbf{a}+\mathbf{r}_1,\sigma}) + (-\hat{c}^\dagger_{\mathbf{j}+4\mathbf{a}+\mathbf{r}_3,\sigma} - b\hat{c}^\dagger_{\mathbf{j}+3\mathbf{a}+\mathbf{r}_2,\sigma} + b\hat{c}^\dagger_{\mathbf{j}+3\mathbf{a}+\mathbf{r}_4,\sigma}) \\ & + \; (\hat{c}^\dagger_{\mathbf{j}+5\mathbf{a}+\mathbf{r}_3,\sigma}) + ... \end{aligned} \quad \text{(A7)}$$

The fourth $\hat{B}^{\dagger}_{\mu_4,\sigma}$ operator is obtained from (A7) by translating the starting point of the period with one cell, i.e. taking $\mathbf{Z}_{j+1} = \mathbf{Z}^e_2$. One gets

$$\begin{aligned}\hat{B}^{\dagger}_{\mu_4,\sigma} &= ... + (-\hat{c}^{\dagger}_{\mathbf{j}+\mathbf{a}+\mathbf{r}_3,\sigma} - b\hat{c}^{\dagger}_{\mathbf{j}+\mathbf{r}_2,\sigma} + b\hat{c}^{\dagger}_{\mathbf{j}+\mathbf{r}_4,\sigma}) + (\hat{c}^{\dagger}_{\mathbf{j}+2\mathbf{a}+\mathbf{r}_3,\sigma}) \\ &+ (-\hat{c}^{\dagger}_{\mathbf{j}+3\mathbf{a}+\mathbf{r}_1,\sigma} + b\hat{c}^{\dagger}_{\mathbf{j}+2\mathbf{a}+\mathbf{r}_2,\sigma} - b\hat{c}^{\dagger}_{\mathbf{j}+2\mathbf{a}+\mathbf{r}_4,\sigma}) + (\hat{c}^{\dagger}_{\mathbf{j}+4\mathbf{a}+\mathbf{r}_1,\sigma}) \\ &+ (-\hat{c}^{\dagger}_{\mathbf{j}+5\mathbf{a}+\mathbf{r}_3,\sigma} - b\hat{c}^{\dagger}_{\mathbf{j}+4\mathbf{a}+\mathbf{r}_2,\sigma} + b\hat{c}^{\dagger}_{\mathbf{j}+4\mathbf{a}+\mathbf{r}_4,\sigma}) + (\hat{c}^{\dagger}_{\mathbf{j}+6\mathbf{a}+\mathbf{r}_3,\sigma}) + ... \end{aligned} \tag{A8}$$

Continuing the translation by one cell and taking $\mathbf{Z}_{j+2} = \mathbf{Z}^e_2$ one obtains the $\hat{B}^{\dagger}_{\mu_5,\sigma}$ operator as follows

$$\begin{aligned}\hat{B}^{\dagger}_{\mu_5,\sigma} &= ... + (\hat{c}^{\dagger}_{\mathbf{j}+\mathbf{a}+\mathbf{r}_1,\sigma}) + (-\hat{c}^{\dagger}_{\mathbf{j}+2\mathbf{a}+\mathbf{r}_3,\sigma} - b\hat{c}^{\dagger}_{\mathbf{j}+\mathbf{a}+\mathbf{r}_2,\sigma} + b\hat{c}^{\dagger}_{\mathbf{j}+\mathbf{a}+\mathbf{r}_4,\sigma}) \\ &+ (\hat{c}^{\dagger}_{\mathbf{j}+3\mathbf{a}+\mathbf{r}_3,\sigma}) + (-\hat{c}^{\dagger}_{\mathbf{j}+4\mathbf{a}+\mathbf{r}_1,\sigma} + b\hat{c}^{\dagger}_{\mathbf{j}+3\mathbf{a}+\mathbf{r}_2,\sigma} - b\hat{c}^{\dagger}_{\mathbf{j}+3\mathbf{a}+\mathbf{r}_4,\sigma}) \\ &+ (\hat{c}^{\dagger}_{\mathbf{j}+5\mathbf{a}+\mathbf{r}_1,\sigma}) + (-\hat{c}^{\dagger}_{\mathbf{j}+6\mathbf{a}+\mathbf{r}_3,\sigma} - b\hat{c}^{\dagger}_{\mathbf{j}+5\mathbf{a}+\mathbf{r}_2,\sigma} + b\hat{c}^{\dagger}_{\mathbf{j}+5\mathbf{a}+\mathbf{r}_4,\sigma}) + ... \end{aligned} \tag{A9}$$

With $\mathbf{Z}_{j+3} = \mathbf{Z}^e_2$ one obtains the last independent operator generated by $\mathbf{Z}^e_2$, namely $\hat{B}^{\dagger}_{\mu_6,\sigma}$, in the form

$$\begin{aligned}\hat{B}^{\dagger}_{\mu_6,\sigma} &= ... + (-\hat{c}^{\dagger}_{\mathbf{j}+\mathbf{a}+\mathbf{r}_1,\sigma} + b\hat{c}^{\dagger}_{\mathbf{j}+\mathbf{r}_2,\sigma} - b\hat{c}^{\dagger}_{\mathbf{j}+\mathbf{r}_4,\sigma}) + (\hat{c}^{\dagger}_{\mathbf{j}+2\mathbf{a}+\mathbf{r}_1,\sigma}) \\ &+ (-\hat{c}^{\dagger}_{\mathbf{j}+3\mathbf{a}+\mathbf{r}_3,\sigma} - b\hat{c}^{\dagger}_{\mathbf{j}+2\mathbf{a}+\mathbf{r}_2,\sigma} + b\hat{c}^{\dagger}_{\mathbf{j}+2\mathbf{a}+\mathbf{r}_4,\sigma}) + (\hat{c}^{\dagger}_{\mathbf{j}+4\mathbf{a}+\mathbf{r}_3,\sigma}) \\ &+ (-\hat{c}^{\dagger}_{\mathbf{j}+5\mathbf{a}+\mathbf{r}_1,\sigma} + b\hat{c}^{\dagger}_{\mathbf{j}+4\mathbf{a}+\mathbf{r}_2,\sigma} - b\hat{c}^{\dagger}_{\mathbf{j}+4\mathbf{a}+\mathbf{r}_4,\sigma}) + (\hat{c}^{\dagger}_{\mathbf{j}+6\mathbf{a}+\mathbf{r}_1,\sigma}) + ... \end{aligned} \tag{A10}$$

The use of $\mathbf{Z}^e_3$ leads to $\hat{B}^{\dagger}_{\mu,\sigma}$ operators linearly dependent on $\hat{B}^{\dagger}_{\mu_3,\sigma}, \hat{B}^{\dagger}_{\mu_4,\sigma}, ..., \hat{B}^{\dagger}_{\mu_6,\sigma}$.

Further operators $\hat{B}^{\dagger}_{\mu}$ from the eigenvectors of $\tilde{\mathbf{W}}_4$ presented in (A2) cannot be constructed. But the list of new independent $\hat{B}^{\dagger}_{\mu}$ operators can be continued by looking for unity eigenvalues of $\tilde{\mathbf{W}}_n$, $n \neq 4$, and continuing the procedure presented above. For example in the present case $\tilde{\mathbf{W}}_2$ has also unity eigenvalue holding eigenvector with non-zero norm $\mathbf{Z}^e_4$ with properties

$$\mathbf{Z}^e_4 = \begin{pmatrix} 1 \\ 1 \\ 0 \\ 0 \end{pmatrix}, \quad \tilde{\mathbf{R}}\mathbf{Z}^e_4 = \begin{pmatrix} -1 \\ -1 \\ 0 \\ 0 \end{pmatrix}, \tag{A11}$$

leading to following contribution by $\mathbf{Z}_j = \mathbf{Z}^e_4$.

The linear independence of the explicit $\hat{B}^{\dagger}_{\mu,\sigma}$ operators present in (A4,A5,A7 - A10) results from the fact that each of them has a specific (and different) group of missing initial fermionic creation operators.

---

[1] G. A. Mansoori, ,,Principles of Nanotechnology, Molecular-Based Study of Condensed Matter in Small Systems", World Scientific, 2005.

[2] S. K. Shukla, R. I. Bahar, ,,Nano, Quantum and Molecular Computing. Implications to High Level Design and Validation", Kluwer Academic Publishers, 2004.

[3] R. Arita, Y. Suwa, K. Kuroki, H. Aoki, Phys. Rev. Lett. **88**, 127202, (2002).

[4] J. E. Anthony, Angewante Chemie International **47**, 452, (2007).

[5] D. J. Gundlach et al. Nature Materials **7**, 216, (2008).

[6] A. C. R. Grayson et al. Nature Materials **2**, 767, (2003).

[7] J. Ho Cho et al. Nature Materials **7**, 900, (2008).

[8] Z. Gulácsi, A. Kampf, D. Vollhardt, Phys. Rev. Lett. **99**, 026404, (2007).

[9] Z. Gulácsi, A. Kampf, D. Vollhardt, Progr. of Theor. Phys. Suppl. **176**, 1, (2008).

[10] E. Müller-Hartmann, Jour. Low Temp. Phys. **99**, 349, (1995).

[11] S. Daul, R. M. Noak, Phys. Rev. **B58**, 2635, (1997).

[12] M. W. Long et al. Jour. of Phys.: Condens. Matter. **6**, 481, (1994).

[13] A. Mielke, Phys. Lett. **A174**, 443, (1993).

[14] H. Tasaki, Phys. Rev. Lett. **75**, 4678, (1995).

[15] K. Penc et al. Phys. Rev. **B54**, 4056, (1996).

[16] O. Derzhko, A. Honecker, J. Richter, Phys. Rev. **B76**, 220402(R), (2007).

[17] H. K. Kono, Y. Kuramoto, Jour. Phys. Soc. Jpn. **75**, 084706, (2006).

[18] J. Vidal et al. Phys. Rev. Lett. **85**, 3906, (2000).

[19] R. Arita, Y. Suwa, K. Kuroki, H. Aoki, Phys. Rev. **B68**, 140403(R), (2003).

[20] Y. Suwa et al. Phys. Rev. **B68**, 174419, (2003).

[21] Z. Gulácsi, A. Kamfp, D. Vollhardt, in preparation.

[22] M. A. Balds, R. J. Holmes, S. R. Forrest, Phys. Rev. **B66**, 035321, (2002).

[23] S. Yamamoto, Phys. Rev. **B78**, 235205, (2008).

[24] M. Topsakal, E. Aktürk, S. Ciraci, Cond-mat arXiv:0812.4454.

[25] G. Brocks, J. van den Brink, A. F. Morpurgo, Phys. Rev. Lett. **93**, 146405, (2004).

[26] Z. Gulácsi, D. Vollhardt, Phys. Rev. Lett. **91**, 186401, (2003).

[27] Z. Gulácsi, D. Vollhardt, Phys. Rev. **B72**, 075130, (2005).

[28] I. Orlik, Z. Gulácsi, Phil.Mag.Lett. **78**,177,(1998).

[29] Z. Gulácsi, I. Orlik, Jour. of Phys: Math. Gen. **A34**, L359, (2001).

[30] I. Orlik, Z. Gulácsi, Phil. Mag. **B81**, 1587, (2001).

[31] Z. Gulácsi, Eur. Phys. Jour. **B30**, 295, (2002).

[32] P. Gurin, Z. Gulácsi, Phys. Rev. **B64**, 045118, (2001).

[33] Z. Gulácsi, Phys. Rev. **B66**, 165109, (2002).

[34] Z. Gulácsi, Phys. Rev. **B69**, 054204, (2004).

[35] L. G. Sarasua, M. A. Continentino, Phys. Rev. **B65**, 233107, (2002); ibid. **B69**, 073103, (2004).

[36] L. G. Sarasua, Phys. Rev. **B75**, 054504, (2007).

[37] Z. Gulácsi, M. Gulácsi, Phys. Rev. **B73**, 014524, (2006).

[38] Z. Gulácsi, Phys. Rev. **B77**, 245113, (2008).

[39] D. J. Klein, J. Phys. A: Math. Gen. **15**, 661, (1982); Z. Nussinov, A. Rosengren Phil. Mag. Lett. **87**, 515 (2007).

[40] E. Kovács, Z. Gulácsi, Jour. of Phys. **A38**, 10273, (2005).

[41] A. H. Castro Neto et al. Rev. Mod. Phys. **80**, no:4 (2008) under press (cond-mar arXiv:0709.1163).

[42] E. H. Lieb, F. Y. Wu, Phys. Rev. Lett. **20**, 1445 (1968).

[43] I. Chalupa, Z. Gulácsi, Jour. of Phys. **C19**, 386209, (2007).

[44] These conditions represent only a restriction of the parameter space into a domain where the example of the Appendix A is present.